Naguleswaran, Sanjeevan; Chakrawarthy, R. S.; Garg, U.; Lamkin, K. L.; Smith, Geoff; Walpe, J. C.; Galindo-Uribarri, A.; Janzen, V. P.; Radford, D. C.; Kaczarowski, R.; Fossan, D. B.; Lafosse, D. R.; Vaska, P.; Droste, C.; Morek, T.; Pilotte, S.; DeGraaf, J.; Drake, T.; Wyss, R.

Magnetic and intruder rotational bands in ^{113}In Physical Review C, 2005; 72(4):044304

http://link.aps.org/doi/10.1103/PhysRevC.72.044304

Magnetic and intruder rotational bands in ^{113}In

S. Naguleswaran,[1,*] R. S. Chakrawarthy,[2] U. Garg,[1] K. L. Lamkin,[1] G. Smith,[1] J. C. Walpe,[1] A. Galindo-Uribarri,[3,†] V. P. Janzen,[3] D. C. Radford,[3,†] R. Kaczarowski,[4] D. B. Fossan,[5] D. R. Lafosse,[5] P. Vaska,[5] Ch. Droste,[6] T. Morek,[6] S. Pilotte,[7] J. DeGraaf,[8] T. Drake,[8] and R. Wyss[9]

[1]*Physics Department, University of Notre Dame, Notre Dame, Indiana 46556, USA*
[2]*TRIUMF, 4004 Wesbrook Mall, Vancouver, British Columbia V6T 2A3, Canada*
[3]*Chalk River Nuclear Laboratories, AECL Research, Chalk River, Ontario K1J 1J0, Canada*
[4]*Soltan Institute of Nuclear Studies, 05-400 Swierk, Poland*
[5]*Department of Physics, State University of New York, Stony Brook, New York 11794, USA*
[6]*Institute of Experimental Physics, Warsaw University, ul. Hoza 69, 00-681 Warsaw, Poland*
[7]*Department of Physics, University of Ottawa, Ottawa, Ontario K1N 6N5, Canada*
[8]*Department of Physics, University of Toronto, Toronto, Ontario M5S1A7, Canada*
[9]*Royal Institute of Technology, KTH, Alba Nova Centre, Stockholm, Sweden*

(Received 1 April 2005; published 13 October 2005)

Excited states in ^{113}In were populated via the reactions ^{100}Mo(^{18}O,$p4n$)^{113}In and ^{110}Pd(^{7}Li,$4n$)^{113}In. The two known $\Delta J = 2$ intruder bands, based on the $\pi g_{7/2} \otimes d_{5/2}$ and $\pi h_{11/2}$ orbitals, have been extended by $8\hbar$ to spins $(49/2^{+})\hbar$ and $(55/2^{-})\hbar$, respectively. The previous finding of three sequences of $\Delta J = 1$ γ-ray transitions has been confirmed. A self-consistent cranked shell-model calculation gives a good description of the contrasting alignment patterns of the two $\Delta J = 2$ intruder bands. The intruder bands, the known sequences of $M1$ transitions, and spherical levels together represent a coexistence of three different excitation modes in this nucleus.

DOI: 10.1103/PhysRevC.72.044304 PACS number(s): 21.10.Re, 27.60.+j, 23.20.En, 23.20.Lv

I. INTRODUCTION

The level structures of nuclei in the Sn region provide a wealth of information on the coexisting deformed bands, spherical structures [1–3], and the nearly spherical magnetic-rotational bands [4–6]. Deformed states in Sn isotopes arise because of the proton particle-hole excitation across the $Z = 50$ shell gap. Thus, the nucleus evolves from a singly closed-shell system to an open shell one in which the protons and neutrons have increased overlap in the $g_{7/2}$, $d_{5/2}$, and $h_{11/2}$ orbitals; this is a well-known mechanism leading to nuclear deformation. The deformed 2p2h states occur at a relatively low excitation energy of $\sim$2 MeV and are based on a deformed prolate configuration, $(\pi g_{7/2})^2 \otimes (\pi g_{9/2})^{-2}$ [1]. In the Indium nuclei, the rotational bands are thought to be based on a particle-hole excitation of the odd-proton across the $Z = 50$ shell gap; additionally, even at moderate rotational frequencies, the strongly β-driving $\pi[550]1/2^{-}$ Nilsson orbital is occupied and plays an important role in this mass region [5,6]. Many intruder bands in the Sn region are not linked to states in the known level schemes and, therefore, the spin-parity quantum numbers for these bands and the underlying decay-out mechanisms are yet to be identified [5,6]. High-spin states in In nuclei near the $N = 66$ midshell region are largely unexplored, primarily because of the lack of suitable reactions in which these nuclei are the dominant reaction products. As a part of our program to systematically study intruder bands in the odd-A In isotopes, we have investigated ^{109,113,115}In nuclei in different experiments [7,8]. Previous work on ^{113}In has resulted in the placement of four sequences of magnetic dipole bands and two intruder bands [6]; the observed bands have been suggested as arising because of a coupling of the neutrons in the normal-parity and unique-parity orbitals with the odd-$g_{9/2}$ proton and, upon its excitation across the $Z = 50$ shell gap, to the orbitals in the next oscillator shell, giving rise to magnetic-dipole bands and intruder bands, respectively [6]. The magnetic dipole bands in In nuclei are unique in the sense that their angular-momentum extent is rather limited and, importantly, do not involve the $Z \sim 50$ proton-core excitation, unlike the long cascades of $M1$ γ-ray transitions in the Pb region that involve the breaking of the $Z = 82$ closed core [9].

In the present article we report on the γ-ray spectroscopy of ^{113}In. We have confirmed the earlier observation of three sequences of $\Delta J = 1$ magnetic dipole bands [6] and have extended, by $8\hbar$, the two known $\Delta J = 2$ decoupled rotational bands. The contrasting alignment patterns of the two bands have been examined within the framework of a Cranked Shell model calculation which includes, in addition, quadrupole pairing. Part of this work has been reported previously [10].

II. EXPERIMENT AND RESULTS

In two different experiments, states in ^{113}In were populated with the reactions, ^{100}Mo(^{18}O,$p4n$)^{113}In (performed at AECL, Chalk River, Canada) and ^{110}Pd(^{7}Li,$4n$)^{113}In (performed at the Notre Dame Nuclear Structure Laboratory) at beam energies

*Present address: School of Electrical, Electronics Engineering, The University of Adelaide, SA 5005, Australia.
†Present address: Physics Division, Oak Ridge National Laboratory, Oak Ridge, TN 37831, U.S.A.

of 95 and 36 MeV, respectively. At Notre Dame, the low spin states were populated in a ^{7}Li-induced reaction on a 0.5 mg/cm^2 thick, self-supporting foil of enriched ^{110}Pd. The emitted γ-rays were detected with an array of five Compton-suppressed high-purity germanium detectors, placed at angles of 30°, 90°, 150°, 270°, and 330° with respect to the beam axis. Approximately 8 million $\gamma\gamma$ coincidences were acquired and written to tape.

In the Chalk River experiment, the target consisted of two self-supporting foils of ^{100}Mo, each 0.3 mg/cm^2 thick. The ^{18}O beam was provided by the Tandem Accelerator Superconducting Cyclotron (TASCC) facility. The emitted γ rays were detected with the 8π spectrometer that comprised 20 Compton-suppressed high-purity germanium detectors (CS-HPGe) and a 4π spherical shell consisting of 71 Bismuth Germanate (BGO) detectors. The spectrometer was employed in conjunction with a 96-element CsI charged particle detector array to acquire multiplicity-particle-γ-γ coincidences; the BGO ball provided information on γ-ray sum-energy and multiplicity. Each HPGe detector had an efficiency of approximately 25% of the standard 7.6 × 7.6 cm NaI(Tl) crystal (at 1.33 MeV). The gains of CS-HPGe detectors were adjusted online for the recoil velocity ($v/c \sim 1.5\%$). Events in which two or more CS-HPGe detectors fired in prompt time coincidence with eight or more elements in the BGO inner ball were written to tape. In all, about 3.6×10^8 γ-γ coincidence events were accumulated, of which the $p4n$ reaction exit channel, leading to states in ^{113}In, comprised about 10%. Standard γ-ray sources were used to obtain the efficiency calibrations in both the experiments. The coincidence data were gain matched and sorted offline into 2k × 2k E_γ-E_γ matrices, as well as charged-particle-gated 2k × 2k, E_γ-E_γ matrices. Coincidences with the charged particle CsI array were decisive in establishing the high-spin structure in this weakly populated exit channel. Data analysis was facilitated by the ESCL8R software [11].

A partial level scheme for ^{113}In, derived from the two experiments, is presented in Fig. 1. The level scheme is based on coincidence relationships and relative intensities obtained from the two sets of matrices described above. Spin assignments are based on (i) directional correlation analysis, (ii) known spins of band-head states from previous works, (iii) the assumption that spin values increase with excitation energy, and (iv) model expectations for the population of the favored-signature states of decoupled rotational bands. For the DCO analysis, two sets of matrices were constructed: One set involved coincidences between the detectors at 37° and 79°, and the other between the detectors at 37° and 143°. When gated by γ-ray transitions in the set of detectors at 37°, the ratio of the projected γs between the two sets of matrices was close to 1.2 for stretched $\Delta J = 2$ γ-ray transitions and close to 0.8 for the $\Delta J = 1$ transitions; the ratio calibration was done using known γ-ray transitions. Grouping of several CS-HPGe detectors into rings of fewer angles is possible as the 8π γ-detector array is highly symmetric.

Previous experiments using light ions had established many levels up to about 6 MeV in excitation energy [6,12]. The present data analysis, with a few minor differences, confirms most of these proposed levels and extends the known level scheme to higher spins. The two most intense bands, labeled band 1 and band 2 in Fig. 1, are known to decay mainly through the 888-, 1324-, and 938-keV γ-ray transitions, respectively, populating the $13/2^+$ state at 1.344 MeV. We confirm the level ordering of the intensely populated members of band 1, which are the 163-, 267-, 189-, 169-, and 256-keV γ-ray transitions. A short cascade of mutually coincident sequence, consisting of 474-, 340-, 379-, and 362-keV γ-ray transitions, was inferred to feed levels of band 1 at the $31/2^-$ and $29/2^-$ levels, though the linking γ-ray transitions could not be established; in Ref. [6] the 474-keV γ-ray transition is assigned to belong to ^{113}In, but not placed. Members of band 2 are the known 183-, 391-, 589-, 685-, 727-, and 558-keV (new) γ-ray transitions. Detection of the previously deduced, but unobserved, 50-keV γ-ray transition and the reported 92-keV γ-ray transition could not be confirmed as the HPGe detector thresholds were set to 100 keV in both the experiments. The DCO values for members of bands 1 and 2 are between 0.6 and 0.7, confirming their dipole multipolarity. In band 1, observation of the $\Delta J = 2$ crossover $E2$ transitions confirms the $M1$ character of the 692-, 742-, and 677-keV γ-ray transitions. Similar $\Delta J = 2$ crossover transitions, reported in Ref. [6], could not be observed in band 2. The present work confirms most of the yrast γ-ray transitions but the sensitivity to locate yrare transitions, reported in Ref. [6], is rather limited.

The analysis of the coincidence data from Chalk River has revealed a coincident cascade comprising the known 507-, 572-, 696-, 818-, 928-, 1028-keV γ-ray transitions and, in addition, the 1122-, 1212-, 1294-, and 1396-keV new γ-ray transitions. Figure 2 displays the sum of background-subtracted coincidence spectra gated by the 572-, 818-, and 928-keV γ-ray transitions; a typical rotational sequence is evident. Based on relative intensities and coincidence relationships, these transitions have been assigned to band 3. The nine $\Delta J = 2$ $E2$ γ-ray transitions extend band 3 to a J^π value of $(59/2^-)$, $8\hbar$ higher than the previous work [6]. The γ-ray transitions of band 3 were found to be in coincidence with the previously known low-lying levels; in particular, the clear observation of 1344-, 888-, and 1191-keV γ-rays in the coincidence spectrum unambiguously places this band in ^{113}In. The positive-parity rotational band (band 4 in Fig. 1), based on the $7/2^+$ level, consists of the previously known 497-, 699-, 803-, 773-, 638-keV stretched $E2$ γ-ray transitions, as well as the new 708-, 916-, 1061-, and 1147-keV γ-ray transitions, extending the band to a J^π value of $(43/2^+)$. A sum-gated spectrum is shown in Fig. 3. The spin assignments of the relatively intensely populated members of these rotational bands are based on a DCO analysis, as well as the angular distribution data from the earlier work [6].

Coincidence data suggests feeding of members of band 3 to the known levels at 2232 $(15/2^-)$ and 2395 keV $(17/2^-)$ through the 408- and a 572-keV (a doublet) γ-ray transitions. Addtionally, the presence of the 1191-keV γ-ray transition in the gated spectrum (Fig. 2) suggests decay paths to the positive-parity intruder band (band 4 in Fig. 1); indeed, a 671-keV γ-ray transition was deduced to be in coincidence with members of band 3, as well as with the 497- and 1191-keV γ-ray transitions, which are members of band 4; firm decay paths to these levels could not be found, however. In agreement with the previous work [6], we infer that the 377- and 457-keV

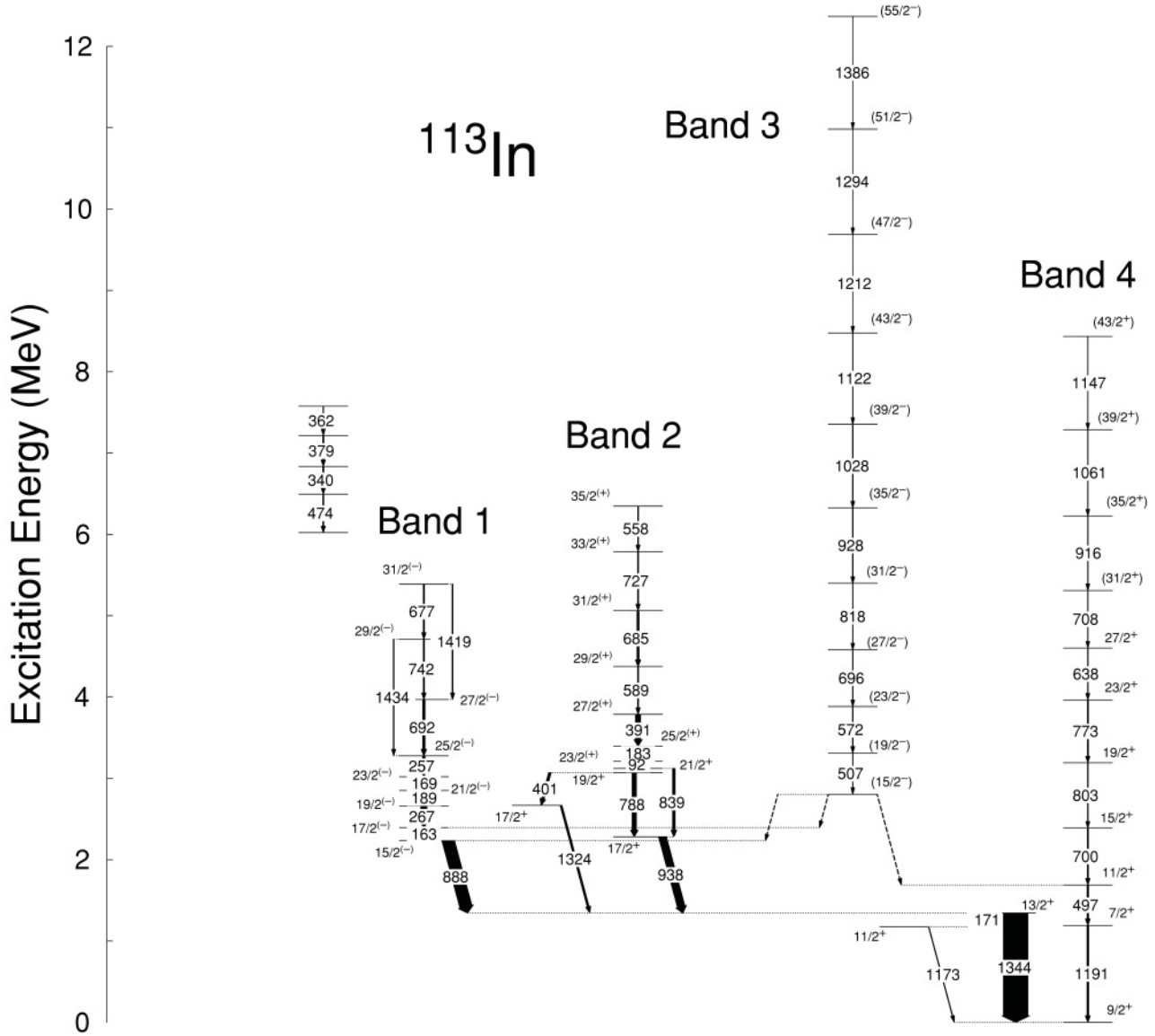

FIG. 1. The level scheme of ^{113}In from the present experiment. γ-ray transition energies are marked in kilo-electron volts. Decay paths of band 3 are indicated by dotted arrows.

γ-ray transitions might be involved in the decay-out of the band. The present experiment is not sensitive to detect low energy γ-ray transitions; however, as per the inset of Fig. 7 of Ref. [6], several unlabeled peaks are evident at low energies, hinting at a fragmented decay path via low energy γ-ray transitions as well. Clearly, there exist other decay pathways, well below the detection threshold of the present experiment. The quadrupole nature of the 507- and 572-keV γ-ray transitions is deduced from an angular distribution analysis reported in an earlier study [6] and the present DCO analysis, which includes the contribution from the second 572-keV transition as well. We have assigned $J^{\pi} = (15/2)^{-}$ to the lowest level of band 3 on the basis of comparison with aligned angular momentum of such intruder bands in ^{111}In [5] and ^{113,115}Sb nuclei [13,14]. A J^{π} assignment of $19/2^{-}$ would lead to an additional $2\hbar$ of alignment that cannot be explained and is, therefore, ruled out. The present analysis leads to different, but more realistic, spin assignments than those in Ref. [6]. The very large signature splitting between the two signature partners of the $\pi h_{11/2}$ orbital suppresses the population of the unfavored band, based on a $17/2^{-}$ state, and can therefore be excluded; indeed, data systematics almost always exclude the possibility of the unfavored signature partner being yrast.

III. DISCUSSION

The physics of the low-spin states in In isotopes has been a subject of extensive studies in which the structure of these nuclei has been described within the framework of particle $\otimes$ Cd-core or, equivalently, in a hole $\otimes$ Sn-core model [15]. Magnetic dipole bands in $^{107-113}$In isotopes have

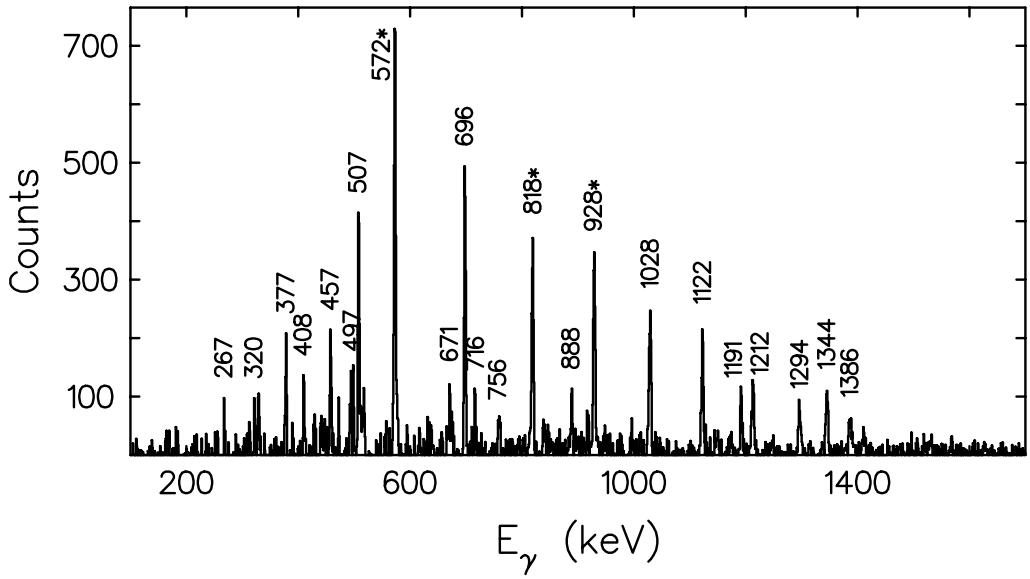

FIG. 2. Sum of γ-ray spectra gated by the members of the band 3. Gating transitions are marked with an asterisk symbol.

been interpreted as shears bands in several articles [5,6,9], including the experimental results from the present work and therefore are not discussed here. Rotational bands in odd-In nuclei arise because of the excitation of the odd-proton to the $g_{7/2}$, $d_{5/2}$, $d_{3/2}$, $s_{1/2}$, and $h_{11/2}$ orbitals. Of these, the ones based on a high-j orbital are yrast and are usually populated in heavy-ion fusion-evaporation experiments. The two $\Delta J = 2$ rotational bands (bands 3 and 4 in Fig. 1) have been previously suggested to be decoupled rotational bands based on the favored signature partner of the $\pi h_{11/2}$ and $\pi g_{7/2} \otimes d_{5/2}$ orbitals, respectively [6]. In the present work, both the bands have been followed to high spins. To gain an insight into the alignment process, first reported in Ref. [6], and the nature of alignining particles at high spins, we have performed calculations based on an extended total routhian surface (TRS) formalism. The self-consistent extended TRS calculations are based on a Woods-Saxon potential incorporating both the monopole and quadrupole pairing, with an additional feature of approximate particle-number projection using the Lipkin-Nogami procedure [16]. The monopole pairing strength is determined by the average gap method, whereas the strength of the quadrupole pairing force stems from the requirement of restoring local Galilean invariance of the system under λ-pole collective shape oscillations and, typically, is 10–20 times weaker than the standard monopole pairing. The total energy is obtained from the macroscopic liquid-drop energy and the

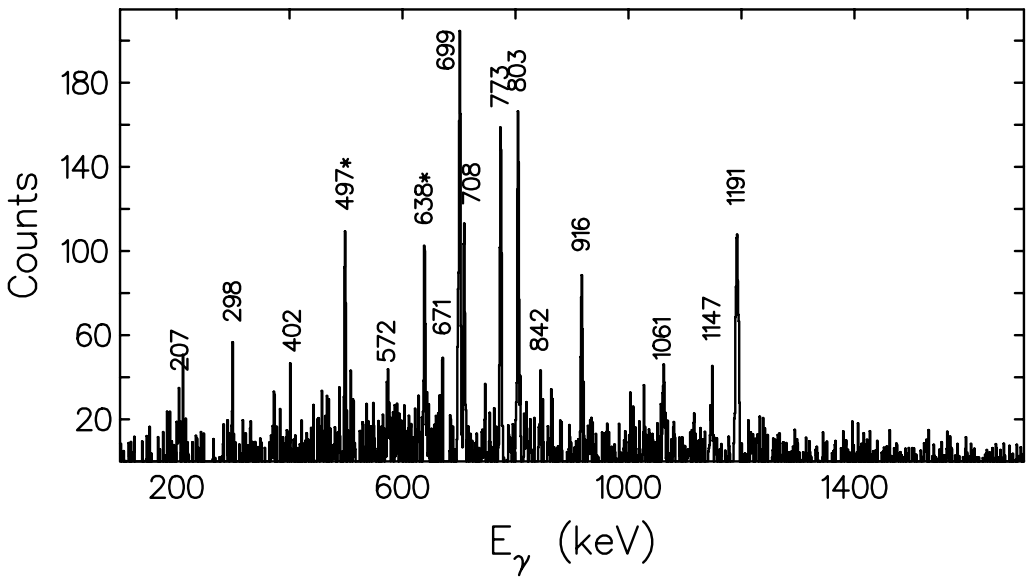

FIG. 3. Sum of γ-ray spectra gated by the members of the band 4. Gating transitions are marked with an asterisk symbol.

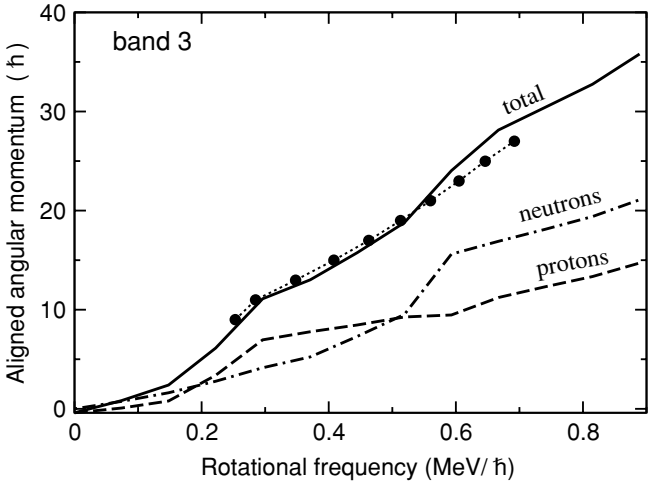

FIG. 4. Experimental data points, connected by a dotted guideline, and the calculated alignment curves for the $\pi h_{11/2}$ band. The dot-dashed and dashed curves correspond to contributions to the aligned angular momentum emanating from the neutrons and proton orbitals, respectively.

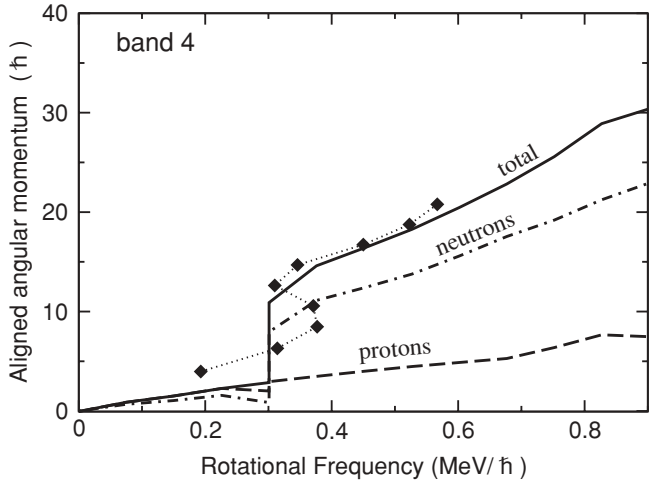

FIG. 5. Experimental data points, connected by a dotted guideline, and the calculated alignment curves for the $\pi g_{7/2}$ band. The dot-dashed and dashed curves correspond to contributions to the aligned angular momentum emanating from the neutrons and proton orbitals, respectively.

Strutinsky shell-correction method [17]. The total energy in the rotating frame is minimized with respect to quadrupole and hexadecapole deformation parameters. The details of this method are described in Ref. [18].

The TRS calculations result in a deformed minimum ($\beta_2 \sim 0.21$, $\gamma \sim 6.4^\circ$), based on the favoured signature of the $\pi h_{11/2}$ orbital, being yrast at a rotational frequency of 0.445 MeV/$\hbar$. The experimental data and calculated alignment curves are depicted in Fig. 4. The composition of the total alignment because of the constituents, mainly the $h_{11/2}$ proton and neutron quasiparticles is also shown in the same figure. The alignment gain, deduced after subtracting a reference rotor, is about 8$\hbar$, but features of backbend are absent. The TRS calculations give a very good account of the observed gradual $\nu h_{11/2}$-alignment pattern; this gradual alignment suggests a large interaction between the 1- and 3-qp bands. In addition, the calculations predict a gradual evolution in the quadrupole deformation parameters, (β_2, γ), from (0.275, 13.2°) at low frequencies to (0.289, 33.7°) at a rotational frequency of 0.89 MeV/$\hbar$, thus evolving to a more triaxial shape. Between rotational frequencies of 0.2 and 0.6 MeV/$\hbar$, the configuration of this band is deduced to be $\pi h_{11/2} \otimes \pi g_{9/2}^{-2} \otimes \nu h_{11/2}^{2}$; whereas at higher frequencies small alignment because of the $g_{9/2}$ protons seems to play a role.

The positive-parity rotational band starting at 1192 keV has been suggested to be based on the favored signature partner of the $\pi g_{7/2}$ orbital; the configuration of this band is known to be based on a proton 1p-2h excitation across the $Z = 50$ shell gap [6]. The TRS calculations result in a deformed minimum ($\beta_2 \sim .21$, $\gamma \sim -3.8^\circ$), based on the favored signature of the $\pi g_{7/2} \otimes d_{5/2}$ orbital, being yrast at a rotational frequency of 0.3 MeV/$\hbar$. The occurrence of this structure is regulated by the crossing between the "extruder" $\pi g_{9/2}$ and the "intruder" ($\pi g_{7/2} \otimes d_{5/2}$) orbitals at a moderate deformation value of $\beta_2 \sim 0.2$ [19]. The observed backbend (cf. Fig. 5) suggests a sharp band crossing, unlike that of band 3, and is indicative of a relatively small interaction between the aligned and the nonaligned structures. The gain in alignment of 8$\hbar$ (with respect to a reference rotor) is attributed to the alignment of neutrons in the $h_{11/2}$, as well as $g_{7/2} \otimes d_{5/2}$ orbitals. The lowest band crossing in these nuclei is always because of the $h_{11/2}$ neutrons and alignments because of other quasiparticles typically occur at frequencies greater than 0.5 MeV/$\hbar$; therefore, the first backbend, observed at ~0.3–0.4 MeV/$\hbar$, is because of $h_{11/2}$ neutrons. The crossing frequency is close to the expected value for a $\nu h_{11/2}$ alignment. [In the $N = 64$ isotone ^{114}Sn [20], for example, this alignment occurs at a frequency of ~0.4 MeV/$\hbar$; the small difference could be because of different core deformations.] As the neutron Fermi surface is close to middle of the $h_{11/2}$ subshell, a $\nu h_{11/2}$ alignment can account for at most 6$\hbar$ of the observed gain in alignment; a small upbend is indeed discernible at frequencies greater than ~0.5 MeV/$\hbar$, which is attributed to the alignment of neutrons in the normal-parity $g_{7/2} \otimes d_{5/2}$ orbitals. In Fig. 5, the TRS calculations described above give a very good account of the observed sharp $\nu h_{11/2}$-alignment pattern; in addition, the model calculations predict a gradual change in the quadrupole deformation parameters, (β_2, γ), from (0.13, −5.2°) at very-low frequencies to (0.21, −3.8°) at a rotational frequency of 0.31 MeV/$\hbar$ and finally evolving to a lower deformation value of (0.17, −0.2°) at 0.8 MeV/$\hbar$. Between rotational frequencies of 0.3 and 0.6 MeV/$\hbar$, the configuration of this band is deduced to be $\pi g_{7/2} \otimes d_{5/2} \otimes \pi g_{9/2}^{-2} \otimes \nu h_{11/2}^{2}$. Despite the involvement of the $Z = 50$ proton core excitation, an essential mechanism to realize deformed bands in this region, it is remarkable that this structure occurs at a lower excitation energy than the corresponding Sn 2p2h band (~2 MeV) across a wide range of In isotopes, *viz.* ^{111}In (1.5 MeV) [5], ^{115}In (934 keV), ^{117}In (748 keV), ^{119}In (721 keV), and ^{121}In (988 keV) [21]. This feature suggests a reduction of proton pairing in these bands.

Previous studies, which included monopole pairing only, have reported difficulties in correctly describing the alignment and, therefore, the moment of inertia of bands (especially band 3), when the constituent protons and neutrons occupy similar orbitals. This is more so when the $h_{11/2}$ orbital, which dictates the high-spin spectra in a large number of nuclei in the $A \sim 100$–130 region [22], is involved. To explain the difference, a residual neutron-proton interaction was invoked and was suggested to play a key role in describing the alignment process. However, within the extended TRS formalism, *both* the quadrupole pairing and a slightly larger deformation (because of the $\pi h_{11/2}$ orbital) seem to be responsible for the observed feature; explicit inclusion of residual neutron-proton interaction, conversely, can explain only a small part of the alignment [18]. Finally, the clear absence of a gradual alignment in the calculations for the normal-parity band (band 4) is a remarkable feature.

IV. CONCLUSIONS

In summary, the high-spin regime in ^{113}In is dominated by two $\Delta J = 2$ rotational bands. TRS calculations explain the contrasting $\nu h_{11/2}$ alignment patterns in these two bands. Together with the earlier data [6], shape-coexistence of three different excitation modes is evident in ^{113}In. The decay-out of the $\pi h_{11/2}$ intruder band in the $N = 64,66$ Sb isotopes [14,20] occurs because of a mixing with the spherical levels. Such level mixing is a generic band-decay-out mechanism in several nuclei, and could well be the case in ^{113}In as well. There are clear indications in the data that some of the decay-out flux in ^{113}In proceeds via potentially new states, which could be accessed in a high-resolution and high-statistics backed-target experiment (as opposed to a self-supporting target, employed in the present series of experiments), and is clearly needed to map the complete decay-out flux of the band. Because of the restrictive target-projectile combinations available, band 3 could not be followed to very high spins, where features such as smooth band-termination are expected to occur. However, with the recent availability of beam-wobbler technology, it might be possible to use thin targets of ^{82}Se with a beam of ^{37}Cl to look for states close to the band-terminating region in the α2n exit channel leading to high spin states in ^{113}In. [Such a system can withstand higher beam intensities on thin ^{82}Se targets, which are known to be very volatile at moderate beam currents.] The determination of level-lifetimes, to test the deformation parameters borne out in the TRS calcualtions, and the elucidation of the complete decay-out path is a subject for further investigations. Experiments with large γ-detector arrays are clearly warranted to realize these expectations and, additionally, to test model predictions of pure magnetic rotation in band 2 [9].

ACKNOWLEDGMENTS

We thank Professor J.C. Waddington and Professor S. Frauendorf for useful discussions. One of us (RSC) is grateful to the University of Notre Dame for hospitality during his stay there. We are grateful to the personnel at TASCC AECL, Chalk River, Canada, and Notre Dame, for smooth operation of the machines during the experiments. This work has been supported in part by the U.S. National Science Foundation, the Natural Sciences and Engineering Council of Canada, and the Maria Sklodowska-Curie Joint Fund II.

[1] J. Bron, W. H. A. Hesselink, H. Bedet, H. Verheul, and G. Vanden Berghe, Nucl. Phys. **A279**, 365 (1977); J. Bron, W. H. A. Hesselink, A. van Poelgest, J. J. A. Zalmstra, M. J. Uitizinger, H. Verheul, K. Heyde, M. Waroquier, H. Vincx, and P. van Isacker, Nucl. Phys. **A318**, 335 (1979).

[2] A. Van Poelgeest, J. Bron, W. H. A. Hesselink, K. Allart, J. J. A. Zalmstra, M. J. Uitzinger, and H. Verheul, Nucl. Phys. **A346**, 70 (1980).

[3] J. L. Wood, K. Heyde, W. Nazarewicz, M. Huyse, and P. van Duppen, Phys. Rep. **102**, 291 (1983).

[4] R. M. Clark and A. O. Macchiavelli, Annu. Rev. Nucl. Sci. **50**, 1 (2000).

[5] P. Vaska *et al.*, Phys. Rev. C **57**, 1634 (1998).

[6] R. S. Chakrawarthy and R. G. Pillay, Phys. Rev. C **55**, 155 (1997).

[7] S. Naguleswaran, Ph.D. thesis, University of Notre Dame (1996) (unpublished);

[8] S. Naguleswaran *et al.*, Z. Phys. A **359**, 235 (1997).

[9] S. Frauendorf and J. Rief, Nucl. Phys. **A621**, 736 (1997); S. Frauendorf, Rev. Mod. Phys. **73**, 463 (2001).

[10] S. Naguleswaran *et al.*, Bull. Am. Phys. Soc. **40**, 1615 (1995).

[11] D. C. Radford, Nucl. Instrum. Methods Phys. Res. A **361**, 297 (1995).

[12] W. K. Tuttle, P. H. Stelson, R. L. Robinson, W. T. Milner, F. K. McGowan, S. Raman, and W. K. Dagenhart, Phys. Rev. C **13**, 1036 (1976); Jean Blachot, Nucl. Data Sheets **104**, 791 (2005).

[13] V. P. Janzen, H. R. Andrews, B. Haas, D. C. Radford, D. Ward, A. Omar, D. Prevost, M. Sawicki, P. Unrau, J. C. Waddington, T. E. Drake, A. Galindo-Uribarri, and R. Wyss, Phys. Rev. Lett. **70**, 1065 (1993).

[14] R. S. Chakrawarthy and R. G. Pillay, Phys. Rev. C **54**, 2319 (1996).

[15] K. Heyde, P. Van Isacker, M. Waroquier, J. L. Wood, and R. A. Meyer, Phys. Rep. **102**, 291 (1983).

[16] W. Satula, R. Wyss, and P. Magierski, Nucl. Phys. **A578**, 45 (1994).

[17] V. M. Strutinsky, Nucl. Phys. **A95**, 420 (1967).

[18] W. Satula, R. Wyss, and F. Dönau, Nucl. Phys. **A565**, 573 (1993); W. Satula and R. Wyss, Phys. Scr. **T56**, 159 (1995).

[19] D. R. LaFosse, D. B. Fossan, J. R. Hughes, Y. Liang, P. Vaska, M. P. Waring, and J.-y. Zhang, Phys. Rev. Lett. **69**, 1332 (1992).

[20] M. Schimmer, S. Albers, A. Dewald, A. Gelberg, R. Wiroswski, and P. von Brentano, Nucl. Phys. **539**, 527 (1992); H. Harada, T. Murukami, K. Yoshida, J. Kasagi, T. Inamura, and T. Kubo, Phys. Lett. **B207**, 17 (1988).

[21] R. Lucas *et al.*, Eur. Phys. J. A **15**, 315 (2002).

[22] S. Frauendorf, J. A. Sheikh, and N. Rowley, Phys. Rev. C **50**, 196 (1994); S. Frauendorf and J. A. Sheikh, *ibid.* **59**, 1400 (1999).